SCIENCE CHINA
Physics, Mechanics & Astronomy

• Article •

February 2012 Vol.55 No.2: 219–223
doi: 10.1007/s11433-011-4595-3

Structure characterization, magnetic and photoluminescence properties of Mn doped ZnS nanocrystalline†

ZUO Ming*, TAN Shun, LI GongPu & ZHANG ShuYuan

Hefei National Laboratory for Physical Sciences at the Microscale, University of Science and Technology of China, Hefei 230026, China

Received June 21, 2011; accepted November 31, 2011; published online December 23, 2011

Wurzite ZnS:Mn nanorods are synthesized via a solvothermal method by using ethylenediamine and water as mixed solvent. The diameters of the nanorods increase and the lengths decrease with the Mn concentration. High resolution transmission electron microscopic images illustrate that a few cubic ZnS:Mn nanoparticles arise along with hexagonal nanorods on high Mn concentration. The samples set off yellow-orange emission at 590 nm, characteristic of $^4T \rightarrow {}^6A_1$ transition of Mn^{2+} at T_d symmetry in ZnS. Electron spin resonance spectrum of the nanorods shows that high Mn concentrations produce a broad envelope, whereas six-line hyperfine appears for lower Mn concentrations. These results together with the magnetization curves indicate that all the ZnS:Mn samples are paramagnetic even down to 4 K, which suggests that the ZnS:Mn is not suitable for dilute magnetic semiconductor.

II-VI semiconductors, nanorods, photoluminescence, magnetic properties

PACS number(s): 61.72.uj, 61.46.km, 78.55.Et, 75.75.+a

Citation: Zuo M, Tan S, Li G P, et al. Structure characterization, magnetic and photoluminescence properties of Mn doped ZnS nanocrystalline. Sci China-Phys Mech Astron, 2012, 55: 219–223, doi: 10.1007/s11433-011-4595-3

ZnS is an important II-VI group compound semiconductor with the widest band gap (E_g~3.7 eV) and is commercially used as optoelectronic and electroluminescent devices. It is suitable for use as host material for a variety of dopants, such as copper-ions [1], manganese-ions [2], iron-ions [3] and has potential application in field emission devices, photoconductors, optical sensors, flat-panel displays and thin film electroluminescence devices [4–8]. Manganese is one of the most common dopants because: (1) it can be incorporated into a ZnS host in large proportions without altering the crystal structure; (2) it has a relatively large magnetic moment and (3) it is electrically neutral in ZnS host, thus avoiding the formation of any acceptor or donor impurities in the crystal [9,10]. Diluted magnetic semiconductors (DMS) are compounds in which magnetic ions (Mn^{2+}, Fe^{2+}, Co^{2+}) are diluted in nonmagnetic II-VI semiconductors (such as ZnO, ZnS, CdS, CdTe, ZnSe, ...). Recently, many efforts have been made for doping of Mn ions into semiconductor [11–13]. However, there are still arguments for the magnetism of the Mn doped II-VI semiconductors. For example, Yoshihiko Kanemitsu group proves that CdS:Mn/ZnS core-shell nanoparticles show paramagnetic behavior [14], while in other literature, ferromagnetic (FM) and antiferromagnetic (AFM) behaviors were reported [15,16].

In this paper, we report a novel solvothermal route to synthesis of ZnS:Mn nanorods with various Mn concentrations. Transmission electron microscopic (TEM) analysis suggests that the crystal structure of ZnS:Mn transfers from hexagonal to cubic at high Mn concentration. Electron spin resonance (ESR) and the magnetization curve indicate that as produced ZnS:Mn samples show paramagnetic behaviour they are not suitable for DMS.

*Corresponding author (email: zuoming@mail.ustc.edu.cn)
†Recommended by ZHANG YuHeng (CAS Academician)

1 Experiments

All of the employed reactants from commercial sources were of analytical grade and were used as received without further purification. An appropriate amount of zinc acetate ($Zn(CH_3COO)_2 \cdot 2.5H_2O$), manganese acetate ($Mn(CH_3COO)_2 \cdot 4H2O$), and thiourea ($NH_2CSNH_2$) powder were placed in the telfon-lined steel autoclave (capacity, 40 mL), which then was filled with ethylenediamine (en)-water mixture (in 2:1 volume ratio). The autoclave was placed in an electric oven at 180°C for 18 h and then cooled to room temperature naturally. The precipitates were centrifuged, washed with de-ionized water and ethanol several times, and dried at 75°C in a vacuum oven for the characterization process.

Power X-ray diffraction (XRD, TTR-III), and high-resolution transmission electron microscopy (HRTEM, JEOL 2010) were used to study the crystal structure and morphology of the products. Photoluminescence (PL) measurements were carried out on a Fluorolog-3-Tau steady-state lifetime spectrophotometer from a Xe lamp at room temperature. Electron paramagnetic resonance study of the powder sample was done with JES-FA200. The magnetization curve was recorded on a Quantium Design SQUID-VSM.

2 Results and discussion

2.1 Structure

The XRD pattern shown in Figure 1 was obtained from the samples with pure ZnS, 1%, 2.5%, 5%, 10%, 20% Mn^{2+} incorporated in ZnS. The XRD spectra reveal that the undoped ZnS sample is crystallized with a pure hexagonal structure. The sharp (002) peak indicates that the ZnS crystal grows in the [001] direction. The crystal structure remains almost the same after Mn^{2+} was doped in ZnS. For the ZnS:Mn (20%) sample, only a tiny peak of cubic ZnS (200) plane appears and this indicates that the sample is a mixture of hexagonal and cubic structure. From this result, it seems that the incorporated Mn^{2+} ions force the transition of ZnS crystal structure.

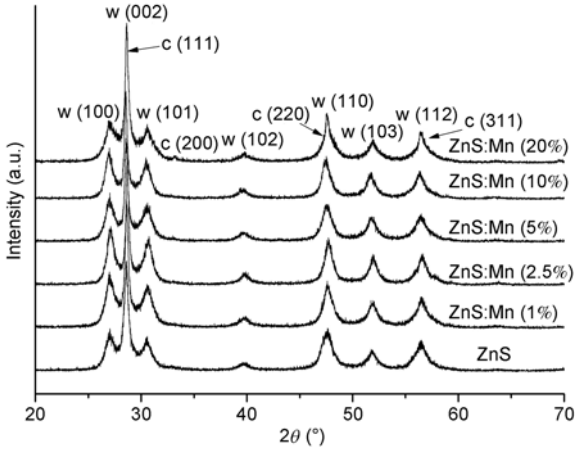

Figure 1 Powder X-ray diffraction pattern of ZnS:Mn nanorods.

In order to investigate the structure change with Mn^{2+} incorporation, TEM and HRTEM experiments were performed. Figure 2(a) shows the TEM image of pure ZnS nanorods. The average diameters and length of undoped ZnS nanorods vary within 10–20 nm and 300–400 nm, respectively. Corresponding HREM image of a single ZnS nanorod is shown in Figure 2(d). Measured lattice spacing is of 0.62 nm and 0.331 nm corresponding to the (001) and (100) plane of hexagonal structure, respectively. The nanorod grows along the [001] direction. With the increase of the Mn concentration, the products are composed of most nanorods and a few nanoparticles. The length of the nanorods decreases and the width increases, while nanoparticles arise and grow much more numerous and bigger. Figure 2(b) and (c) shows the TEM image of ZnS:Mn (10%) and ZnS:Mn (20%) nanocrystalline, respectively. The HRTEM image of nanorods shows that the structure of the nanorods remains the same as pure ZnS nanorod, while the structure of the nanoparticles is quite different. From Figure 2(e), it can be seen that the average diameter of the nanoparicles varies from 5 nm to 10 nm. The lattice spacing of two planes is 0.313 nm and the included angle is 70°. This indicates that the lattice fringe is the (111) plane of cubic ZnS structure with 〈110〉 orientation. In the ZnS:Mn (20%) sample, some bigger nanoparticles with a diameter of 80 nm are found and their HRTEM image is shown in Figure 2(f) with select-area electron diffraction (SAED) in the inset. The spots can be indexed to (111) and (200) of cubic structure with orientation 〈110〉.

For a better understanding of the mechanism of these changes, the energy-dispersive X-ray spectra (EDS) experiments were performed. Atom percentage of Mn in ZnS nanocrystalline is listed in Table 1. For pure ZnS, elemental Zn and S are found in a near stoichiometric ratio with a little Zn deficiency. Table 1 shows that Mn atomic percentage is much less than those actually used during the synthesis process, for example, Mn atom% is 2.08, 3.15 for ZnS:Mn (5%) and ZnS:Mn (20%) nanorods. Mn content in the nanoparticles is found much higher than that in the nanorods. The results indicate that Mn^{2+} ions disperse non-uniformly in ZnS nanocrystallin, a few Mn^{2+} ions enter wurizite ZnS nanorods, and more Mn^{2+} ions intend to assemble together forming a nanocluster in cubic ZnS nanoparticles and therefore restrain the growth of nanorods. Although the exact mechanism behind is not clear, it is supposed that the anions associated with some organic compounds are capable of inducing a phase change from hexagonal to cubic structures in the presence of the organic Mn salt [17].

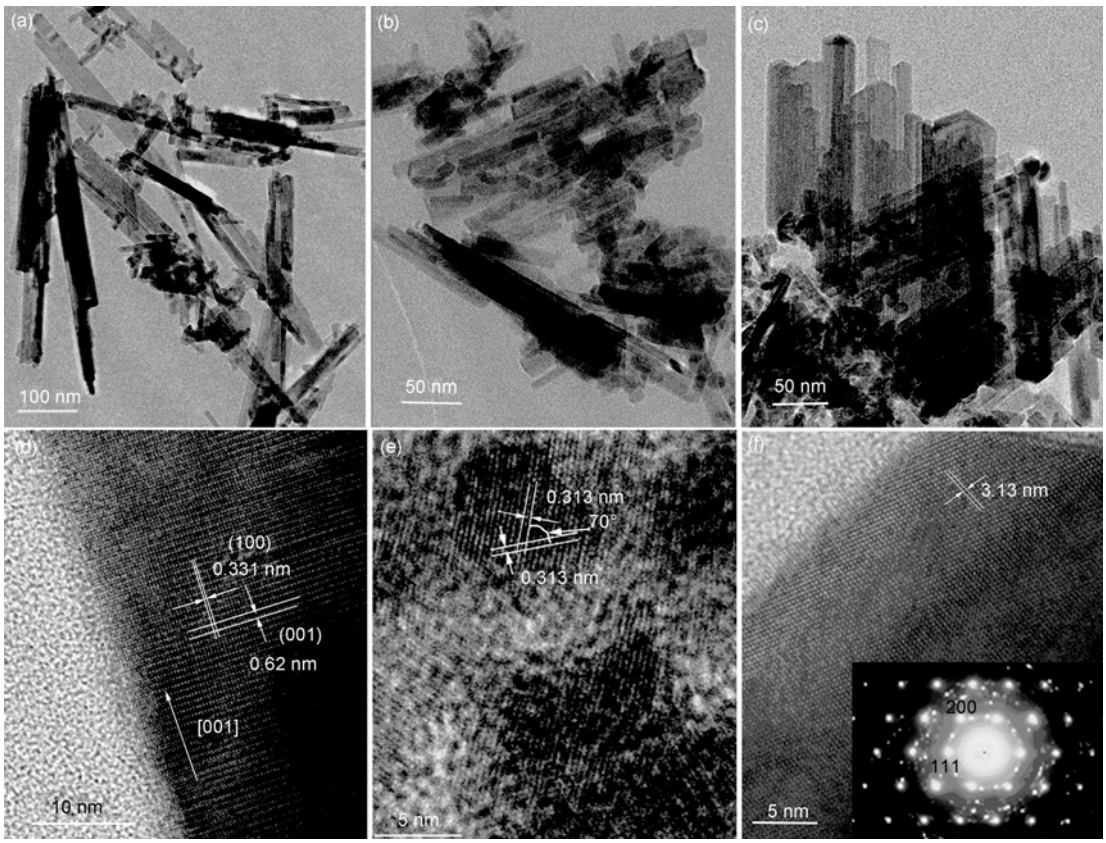

Figure 2 TEM images of the (a) pure ZnS, (b) ZnS:Mn (10%), (c) ZnS:Mn (20%) nanorods; HREM images of (d) ZnS nanorods, (e) ZnS:Mn (10%) nanoparticles and (f) ZnS:Mn (20%) nanoparticles with the corresponding diffraction pattern in the inset.

Table 1 Mn content (atom-percentage) in ZnS nanocrystalline

Mn content	ZnS:Mn (1%)	ZnS:Mn (2.5%)	ZnS:Mn (5%)	ZnS:Mn (10%)	ZnS:Mn (20%)
Nanorod	0.54	1.56	2.08	3.15	3.49
Nanoparticle	–	–	–	7.58	9.19

2.2 Magnetism

ESR measurements were performed to investigate the magnetism of the ZnS:Mn systems. Figure 3(a) shows the ESR spectrum of ZnS nanorods with different Mn infractions recorded by using the microwave of 9000 MHz at room temperature. The spectrum for ZnS:Mn samples is typical for Mn^{2+} ions within II-VI semiconductor compounds [18,19]. This sextet, which is centered at a g-value of g=2, is associated with the allowed (Δm_s=±1, Δm_I=0) magnetic dipolar transitions between the hyperfine-split Zeeman levels of the $^6S_{5/2}$ ground state of the Mn^{2+} 3d-electrons. The hyperfine structure arises from the interaction between the S=5/2 spin of the unpaired 3d-electrons and I= 5/2 spin of the ^{55}Mn nucleus. A close inspection of Figure 3(a) reveals that at low Mn concentration each hyperfine line exhibits super hyperfine lines at the external magnetic field associated with the forbidden transitions. This is typical for Mn^{2+} ions in the environment of a Zn-site in a wurtzite ZnS crystal [20]. For higher Mn concentration, a single broad line is obtained (shown in Figure 3(b)). This is because that the Mn^{2+} ions introduced into the hexagonal ZnS lattice increase to saturation and intend to form Mn clusters in cubic ZnS nanoparticles, causing Mn-Mn atomic distance shorter and the dipole-dipole interaction much stronger, and merging the hyperfine structure into one broad resonance line [21]. All of the ESR results at room temperature indicate that the ZnS:Mn system is paramagnetic. For the sake of investigating the magnetism of ZnS:Mn at lower temperature, ESR experiments at temperature from 5 K to 90 K and M-H curves of ZnS:Mn (20%) were performed. The results of ESR spectra show that the resonance field does not change, suggesting that the system is still in the PM state. With temperature decreasing, the six hyperfine lines reappear, which can be attributed to the suppression of thermal fluctuation. The missing super hyperfine line indicates that the Mn^{2+} ions are located in the cubic ZnS crystal structure whose symmetry is better than the hexagonal structure. The

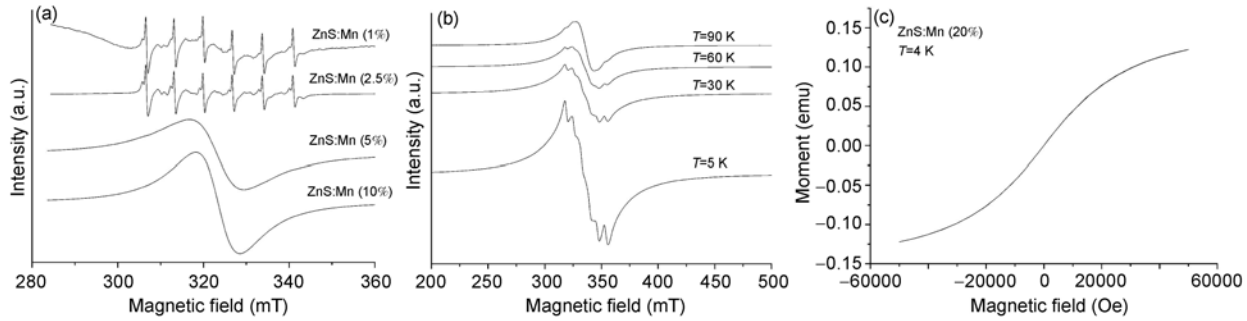

Figure 3 (a) Room temperature ESR spectrum of ZnS:Mn; (b) low temperature ESR spectrum of ZnS:Mn (20%); (c) *M-H* curve of ZnS:Mn (20%) at temperature 4 K.

M-H curve accords with the Langevin equation and no hysteresis is detected, which further confirms that the Mn doped ZnS is paramagnetic even down to 4 K. All these results suggest that the ZnS:Mn is not suitable for dilute semiconductor.

2.3 Photoluminescence properties

Photoluminescence spectra of ZnS:Mn nanorods with a 270 nm excitation wavelength are recorded at room temperature and the result is shown in Figure 4. PL spectrum of the undoped ZnS nanorods (plot a) exhibits one strong green emission peak at 492 nm. The peak at 492 nm is most likely due to the self-activated centers formed by a zinc vacancy in the ZnS lattice [22]. With the increase of Mn concentration, the intensity of green emission decreases. For ZnS:Mn (5%), the green emission completely disappears. Meanwhile, a small orange emission peak at 586 nm arises and becomes dominant and more intense. The orange emission can be attributed to the $^4T_1 \rightarrow {}^6A_1$ transition of Mn^{2+} ions at T_d symmetry in ZnS host [23]. The peak position shifts to a lower energy with increasing Mn content, indicating that the Mn^{2+} concentration is sufficient to influence the crystal-field splitting between the $^4T_1$ and $^6A_1$ states. This behavior indicates that Zinc vacancies are filled with Mn atoms and generate Mn^{2+} photoluminescence centers which result in the quenching of the self-activated emission.

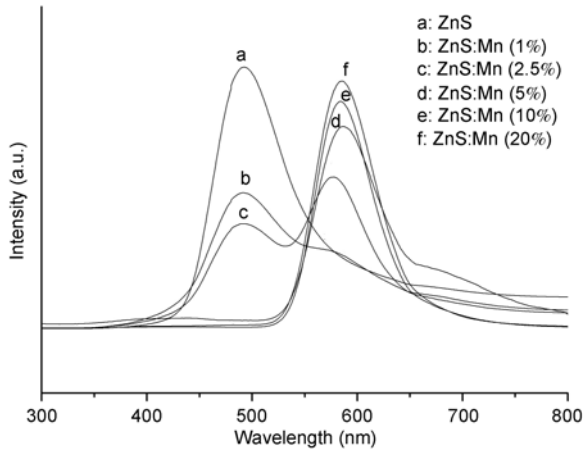

Figure 4 Room temperature PL spectra of ZnS:Mn nanorods.

3 Conclusion

Manganese doped hexagonal ZnS nanorods were synthesized by a solvothermal process. TEM results illuminate that the crystal structure transfers from hexagonal to cubic at high Mn^{2+} concentration. The pure ZnS nanorods exhibit green emissions due to zinc vacancies. Mn doped ZnS nanorods exhibit both green and orange emission at low Mn infraction. Quenching of the green emission at higher Mn infractions is attributed to the vacancy occupation by Mn^{2+} ions. ESR and *M-H* results indicate that Mn^{2+} doped ZnS is paramagnetic and is not an ideal dilute magnetic semiconductor material.

This work was supported by the National Natural Science Foundation of China (Grant No. 50721091).

1 Wang M, Sun L, Fu X, et al. Synthesis and optical properties of ZnS:Cu(II) nanoparticles. Solid State Commun, 2000, 115(9): 493–496
2 Bala P, Valko M, Boldiz E, et al. Properties and reactivity of Mn-doped ZnS nanoparticles. Mater Lett, 2002, 57(1): 188–191
3 Nelkowski H, Pfützenreuter O, Schrittenlacher W. Comparison of luminescence and ESR-investigations in ZnS: Fe. J Liminsci, 1979, 20(4): 403–408
4 Ghosh S C, Thanachayanont C, Dutta J. Studies on zinc sulphide nanoparticles for field emission devices. In: Proceedings of the First ECTI Annual Conference (ECTI-CON 2004), Pattaya, Thailand, 2004. 145–148
5 Garlick J G F, Gibson A F. The luminescence of photo-conducting phosphors. J Opt Soc Am, 1949, 39(11): 935–940
6 Tang W, Cameron D C. Electroluminescent zinc sulphide devices produced by sol-gel processing. Thin Solid Film, 1996, 280(1): 221–226
7 Bredol M, Merikhi J. ZnS precipitation: Morphology control. J Mater Sci, 1998, 33(2): 471–476
8 Falcony C, Garcia M, Ortiz A. Luminescent properties of ZnS:Mn films deposited by spray pyrolysis. J Appl Phys, 1992, 72: 1525–1527

9 Bandaranayake R J, Lin J Y, Jiang H X. Synthesis and properties of $Cd_{1-x}MnxS$ diluted magnetic semiconductor ultrafine particles. J Magn Magn Mat, 1997, 169(3): 289–302

10 Pearce C I, Pattrick, Richard A D, et al. Electrical and magnetic properties of sulfides. Sulfide Mineral Geochem, 2006, 61: 127–180

11 Furdyna J K. Diluted magnetic semiconductors. J Appl Phys, 1988, 64: R29–R65

12 Ohno H. Making nonmagnetic semiconductors ferromagnetic. Science, 1998, 281: 951–956

13 Dietl T, Spalek J. Effect of fluctuations of magnetization on the bound magnetic polaron: Comparison with experiment. Phys ReV Lett, 1982, 48: 355–358

14 Taguchi S, Ishizumi A, Tayagaki T, et al. Mn-Mn couplings in Mn-doped CdS nanocrystals studied by magnetic circular dichroism spectroscopy. Appl Phys Lett, 2009, 94: 173101

15 Nielsen K-W, Philipp J B, Opel M A, et al. Ferromagnetism in Mn-doped ZnO due to impurity bands. Superlattices Microstruct, 2005, 37: 327–332

16 Sandratskii L M, Bruno P. Exchange interactions in ZnMeO (Me=Mn,Fe,Co,Ni): Calculations using the frozen-magnon technique. Phys Rev B, 2006, 73: 045203–045208

17 Hu P A, Liu Y Q, Fu L, et al. Self-assembled growth of ZnS nanobelt networks. J Phys Chem B, 2004, 108: 936–938

18 Lambe J, Kikuchi C. Paramagnetic resonance of CdTe: Mn and CdS: Mn. Phys Rev, 1960, 119: 1256–1260

19 Ishikawa Y. ESR spectra of exchange-coupled Mn^{2+} ions in ZnS and CdS. J Phys Soc Jpn, 1966, 21: 1473–1481

20 Hofmann D M, Hofstaetter A, Leib, U, et al. EPR and ENDOR investigations on CdS: Mn nanocrystals. J Cryst Growth, 1998, 184(2): 383–387

21 Brieler F J, Grundmann P, Fröba M, et al. Formation of $Zn_{1-x}Mn_xS$ nanowires within mesoporous silica of different pore sizes. J Am Chem Soc, 2004, 126(3): 797–807

22 Samelson H, Lempicki A. Fluorescence of Cubic ZnS:Cl, Crystals. Phys Rev, 1962, 125(3): 901–909

23 Sooklal K, Cullum B S, Angel S M, et al. Photophysical properties of ZnS nanoclusters with spatially localized Mn^{2+}. J Phys Chem, 1996, 100(10): 4551–4555